Am J Cancer Res 2023;13(5):2076-2086
www.ajcr.us /ISSN:2156-6976/ajcr0149455

Original Article

The microtubule-targeted agent lisavanbulin (BAL101553) shows anti-tumor activity in lymphoma models

Filippo Spriano[1], Luca Aresu[2], Luciano Cascione[1,3], Giorgia Risi[1], Alberto J Arribas[1,3], Sara Napoli[1], Nicole Forster-Gross[4], Felix Bachmann[4], Marc Engelhardt[4], Heidi Lane[4], Francesco Bertoni[1,5]

[1]Institute of Oncology Research, Faculty of Biomedical Sciences, USI, Bellinzona, Switzerland; [2]Department of Veterinary Science, University of Turin, Grugliasco, Turin, Italy; [3]SIB Swiss Institute of Bioinformatics, Lausanne, Switzerland; [4]Basilea Pharmaceutica International Ltd, Allschwill, Switzerland; [5]Oncology Institute of Southern Switzerland (IOSI), Ente Ospedaliero Cantonale, Bellinzona, Switzerland

Received February 1, 2023; Accepted April 16, 2023; Epub May 15, 2023; Published May 30, 2023

Abstract: Microtubules are major components of the cellular cytoskeleton, ubiquitously founded in all eukaryotic cells. They are involved in mitosis, cell motility, intracellular protein and organelle transport, and maintenance of cytoskeletal shape. Avanbulin (BAL27862) is a microtubule-targeted agent (MTA) that promotes tumor cell death by destabilization of microtubules. Due to its unique binding to the colchicine site of tubulin, differently from other MTAs, avanbulin has previously shown activity in solid tumor cell lines. Its prodrug, lisavanbulin (BAL101553), has shown early signs of clinical activity, especially in tumors with high EB1 expression. Here, we assessed the preclinical anti-tumor activity of avanbulin in diffuse large B cell lymphoma (DLBCL) and the pattern of expression of EB1 in DLBCL cell lines and clinical specimens. Avanbulin showed a potent *in vitro* anti-lymphoma activity, which was mainly cytotoxic with potent and rapid apoptosis induction. Median IC50 was around 10 nM in both ABC and GCB-DLBCL. Half of the cell lines tested showed an induction of apoptosis already in the first 24 h of treatment, the other half in the first 48 h. EB1 showed expression in DLBCL clinical specimens, opening the possibility for a cohort of patients that could potentially benefit from treatment with lisavanbulin. These data show the basis for further preclinical and clinical evaluation of lisavanbulin in the lymphoma field.

Keywords: Lymphoma, EB1, lisavanbulin (BAL101553), microtubule-targeted agent, avanbulin (BAL27862), diffuse large B cell lymphoma (DLBCL)

Introduction

Microtubules are major components of the cellular cytoskeleton. They are ubiquitously found in all eukaryotic cells, and are involved in mitosis, cell motility, intracellular protein and organelle transport, and maintenance of cytoskeletal shape [1]. Microtubules are formed by the polymerization of tubulin into hollow tubes of about 250 Å in diameter. Tubulin in turn is a dimer consisting of α-tubulin and β-tubulin subunits [2, 3]. Tubulin polymerization occurs by a nucleation-elongation mechanism, in which the slow formation of a short microtubule "nucleus" is followed by rapid elongation of the microtubule at its ends by the reversible addition of α- and β-tubulin heterodimers [4]. Microtubules assembly dynamics is a well-regulated process through anchorage on microtubule organizing centers such as centrosomes, and through interaction with a variety of proteins. Microtubule assembly and disassembly occur simultaneously and the net effect, elongation versus shortening, is determined by several factors, including the concentration of free tubulin, chemical mediators such as magnesium and calcium ions and several proteins that interact with unpolymerized tubulin and/or microtubules. Due to their central role in cellular processes, including cellular division, microtubules still represent one of the main targets for anti-cancer therapy [5-7]. In the lymphoma field, successful examples of microtubule-targeted agents (MTAs) are vincristine and vinblas-

tine, part of the R-CHOP and ABVD regimens, respectively, and monomethylauristatin E (MMAE), which is the payload in both brentuximab vedotin and polatuzumab vedotin [5, 8].

Avanbulin (BAL27862) is an MTA characterized by the ability to bind to the colchicine site of tubulin, differently from other MTAs [9], with reported preclinical anti-tumor activity in various solid tumor cell line, including in models resistant to drugs that bind to either the taxane or the vinca alkaloid site on tubulin or that are substrates of the multidrug resistance pump MDR1 [10-14]. Its highly soluble prodrug, lisavanbulin (BAL101553) [15], has entered the initial clinical evaluation with early signs of clinical activity in patients with advanced solid tumors and with recurrent glioblastoma [16-18] and a favorable safety and tolerability profile [19]. Clinical and laboratory data suggest that the anti-tumor activity of avanbulin and of its prodrug lisavanbulin is higher in tumors with strong expression of end-binding protein 1 (EB1) [18, 20, 21], a microtubule-associated protein, important for the regulation of microtubule dynamics [22].

Based on the sensitivity of lymphomas to MTAs, here, we evaluated the *in vitro* activity of avanbulin in diffuse large B cell lymphoma (DLBCL) cell lines and its relationship with expression levels of EB1. The latter was also more extensively studied across datasets of clinical specimens.

Methods

Assessment of anti-lymphoma activity of avanbulin in a panel of lymphoma cell lines

Lymphoma cell lines derived from activated B cell like (ABC) and germinal center B cell type (GCB) DLBCL were exposed to increasing doses of avanbulin. Antiproliferative activity was assessed as previously described [23, 24]. Briefly, cells were manually seeded in 96-well plates at a concentration of 50,000 cells/mL (10,000 cells in each well). Treatments were performed by using the Tecan D300e Digital Dispenser (Tecan, Mannedorf, Switzerland). After 72 hours, cell viability was determined by using 3-(4,5-dimethylth-iazol-2-yl)-2,5-dimethyltetrazolium bromide and the reaction stopped after 4 hours with sodium dodecyl sulfate lysis buffer. The identity of DLBCL cell lines was validated by short tandem repeat DNA fingerprinting [25].

Apoptosis induction and cell proliferation under treatment was evaluated with annexin V staining (AV+) on cells incubated in a live cell imaging system (Incucyte). Ninety-six-well plates coated with 0.01% poly-L-ornithine solution for 1 hour RT and then dried for 30 minutes prior to cell addition. 40,000 cells per well, in a total volume of 100 mL, were seeded. Cells were then treated with four different concentrations of avanbulin (5, 10, 20, 40 nM) or DMSO. Finally, annexin V reagent was added (Incucyte Annexin V Green Dye for Apoptosis) to monitor the apoptosis induction. Each condition was done in triplicate and for each well nine images were taken. Plates were then leaved into the Incucyte Live-Cell Analysis System to monitor apoptosis and cell growth. Images were taken every four hours for a total of 72 hours monitoring. The analysis was performed, with the Incucyte software, in terms of cell growth (cell-by-cell analysis) that allows the counting of the exact number of cells in each image and in terms of apoptosis, counting the number of cells GFP positive during time. Cell growth and number of GFP positive cells was normalized on time 0.

Cell cycle analysis was performed after 24, 48 and 72 h of drug exposure at 20 nM or DMSO. Cells were fixed and permeabilized with ethanol and subsequently stained with propidium iodide. The analyses were performed with the FlowJo software and percentages of cells in G1, S and G2/M phases of the cell cycle were determined.

Transcriptome profiling

Transcriptome profiling of untreated lymphoma cell lines was performed as previously described [26]. For each cell line, 5 millions of cells in exponential growth were collected and resuspended in 1 mL of TRI Reagent (Sigma Aldrich, Buchs, Switzerland) for cell lysis, followed by RNA extraction using the Monarch-Total RNA Miniprep kit (New England Biolabs, Ipswich, MA, USA), according to manufacturer extraction, and genomic DNA digestion. After quality check using the RNA 6000 Nano kit on a BioAnalyzer (Agilent Technologies, Santa Clara, CA, USA), RNA concentration was determined by the Invitrogen Qubit (Thermo Fisher

Scientific) using the RNA BR reagents (ThermoFisher Scientific, Waltham, MA, USA). The cDNA synthesis and addition of barcode sequences was done using the TruSeq RNA Sample Prep Kit v2 for Illumina (Illumina, San Diego, CA, USA) and libraries sequenced via a paired end run on a Illumina NextSeq500, collecting at least 50 millions of reads per sample. The RNA-seq reads quality was evaluated with FastQC (v0.11.5) and removed low-quality reads/bases and adaptor sequences using Trimmomatic (v0.35). The trimmed-high-quality sequencing reads were aligned to the reference genome (HG38) using STAR. The HTSeq-count software package was then used for quantification of gene expression with GENCODE v22 as gene annotation. Data were subsetted to genes that had a counts-per-million value greater than five in at least one cell line. The data were normalized using the 'TMM' method from the edgeR package and transformed to log2 counts-per-million using the edgeR function 'cpm'. Expression values are available at the National Center for Biotechnology Information (NCBI) Gene Expression Omnibus (GEO; http://www.ncbi.nlm.nih.gov/geo) database with accession number GSE221770.

In silico assessment of EB1 in lymphoma clinical specimens and its association with MYC deregulation

We accessed in-silico the association of EB1 and MYC expression in different public datasets of gene expression. We pre-processed individual datasets with ad-hoc pipelines that use the standard de-facto algorithms for the platform used for measuring the mRNA expression levels. In details, for datasets GSE4475 and GSM558119 probe level normalization was done using the calibration and variance stabilization method by Huber et al. [27]. Probeset summarization was performed using the median polish method on the normalized data [28]. For GSE10846, data were analyzed with Microarray Suite version 5.0 (MAS 5.0) using Affymetrix default analysis settings and global scaling as normalization method. The trimmed mean target intensity of each array was arbitrarily set to 500. The raw cel files for GSE98588 were converted into probeset-specific expression values using Affymetrix RMA summarization method as implemented in the BioConductor package simpleaffy [29] using Brainarray custom chip definition files (Version 16) based on Ensemble IDs. For RNA-Seq of our lymphoma cell lines, we evaluated the RNA-seq reads quality with FastQC (v0.11.5) and we removed low-quality reads/bases and adaptor sequences using Trimmomatic (v0.35). The trimmed-high-quality sequencing reads were aligned using STAR [30], a spliced read aligner which allows for sequencing reads to span multiple exons. On average, we were able to align 85% of the sequencing reads for each sample to the reference genome (HG38). The HTSeq-count software package [31] was then used for quantification of gene level expression. We subsetted the data to genes that had a counts-per-million value greater than one in 3 or more samples. The data were normalized per sample using the 'TMM' method from the edgeR package [32], and transformed to log2 counts-per-million using the edgeR function 'cpm'. For TCGA - DLBCL dataset, the alignment step was performed using a two-pass method with STAR. Quality assessment is performed pre-alignment with FASTQC and post-alignment with Picard Tools. Following alignment, BAM files are processed through the RNA Expression Workflow to determine RNA expression levels. The reads mapped to each gene are enumerated using HT-Seq-Count. Expression values are provided in a tab-delimited format. GENCODE v22 was used for gene annotation. RNA-Seq expression level read counts produced by HT-Seq are normalized with the TMM method and log2 transformed (counts-per-million). For the dataset from Schmitz et al. [33], paired-end reads were mapped to the human genome (NCBI build 37) using the gapped aligner STAR using the two-pass method. The alignment file was used for calculating the raw gene expression values by HTseq-count, using the intersection-nonempty model. The counts for gene expression were normalized and log2 transformed using the trimmed-mean (90%) method. For each dataset, we calculated the Pearson correlation coefficient between the normalized expression values for EB1 and MYC.

Immunohistochemistry of DLBCL clinical specimens

Tissue samples from lymphoma clinical specimens prepared as a tissue microarrays (TMA) (LY1001D and LY2086B, TissueArray.

com) were stained for EB1 using a CE-marked immunohistochemistry Clinical Trial Assay (Discovery Life Sciences Biomarker Services GmbH, Kassel Germany). EB1-positivity was quantified by a board-certified pathologist based on the percentage of tumor cells showing moderate or strong staining for EB1, where cellular EB1 staining is defined as: intensity 0 = EB1 staining absent; intensity 1 = weak EB1 staining; intensity 2 = moderate EB1 staining; intensity 3 = strong EB1 staining.

Results

Assessment of anti-lymphoma activity of avanbulin in a panel of lymphoma cell lines

The *in vitro* anti-lymphoma activity of lisavanbulin was assessed in 26 cell lines derived from activated B cell like (ABC; n = 7) and germinal center B cell type (GCB; n = 19) DLBCL. Antiproliferative activity was first evaluated by MTT assay after 72 hours of exposure to increasing concentrations of avanbulin. The compound showed a very high activity in all the cell lines tested, with a median IC50 across cell lines of 11 nM (95% C.I., 10.03-16.17) (**Figure 1A**). No differences were observed based on the cell of origin of the cell lines in terms of IC50 values (ABC, median IC50 10 nM; GCB, 12 nM), nor in terms of AUC (ABC, median AUC 4102, GCB, 4551) (**Figure 1B**, **1C**; Supplementary Table 1).

Cell growth and apoptosis were also monitored using a real-time quantitative live-cell imaging approach in a subset of DLBCL cell lines (n = 17, selected based on their capacity to grow in adherence), treated with DMSO or four different concentrations of avanbulin (5, 10, 20 and 40 nM) compared to untreated cells and images of cell lines were taken every 4 hours for a total of 72 hours. Cell numbers and apoptotic events were measured every 4 hours during a 72 hours period. Most of the cell lines showed a decrease in proliferation after treatment with BAL27862 in line with results obtained with MTT (**Figure 2**; Supplementary Table 2). Apoptosis induction was seen in 15 out of 17 cell lines tested at 20 and 40 nM, and only in one cell line already at 10 nM. Apoptosis could be detected in 8 of 15 cell lines already during the first 24 hours of treatment, while of the remaining cells 6 between 24 and 48 hours in six and after 48 hours in the remaining one (Supplementary Figure 1; Supplementary Table 2).

The activity of avanbulin was correlated with the status of proteins known to be associated with microtubules or involved in MTA sensitivity/resistance such as TP53, BCL2 or MYC [34-37]. We did not observe an association between sensitivity and TP53 or BCL2 status, while based on AUC we identified an association between MYC translocation and sensitivity, with wild type cells more sensitive to the treatment (Supplementary Figure 2; Supplementary Table 3).

Cell cycle experiments were performed in two ABC (OCILY3 and TMD8) and 2 GCB (SUDHL5 and SUDHL16) DLBCL cells at 24, 48 and 72 hours. A strong cytotoxic effect of avanbulin was confirmed with a time-dependent accumulation of cells in sub-G0, starting already at 24 hours in all the four cell lines. A G2-M arrest was also seen in 3 out of 4 cell lines, more evident at 24 hours (Supplementary Figure 3).

Finally, the activity of avanbulin, expressed as IC50, was compared with the activity another microtubulin inhibitor vincristine (Supplementary Figure 4A, 4B). The activity of the two compounds correlates well both comparing internal vincristine data and public data [38]. Overall, vincristine showed a tendency for a higher activity compared to avanbulin (Supplementary Figure 4C, 4D).

EB1 and MYC expression in cell lines

Based on the reported possible association between EB1 expression and sensitivity to avanbulin [18, 20, 21], we evaluated RNA expression in lymphoma cell lines, with no differences between GCB and ABC DLBCL (Supplementary Figure 5). All lymphoma cell lines expressed a high level of EB1. No correlation was observed between expression levels of EB1 and of MYC (Supplementary Figure 5), reported as positively regulated by EB1 in colorectal cancers [22]. When we looked at the possible correlation between EB1 or MYC RNA and protein expression and avanbulin activity, we did not identify any trend for higher sensitivity in EB1 or MYC higher expressing cells comparing low expressors. Most of the cell lines were highly sensitive to avanbulin together with a general high EB1 and MYC expression

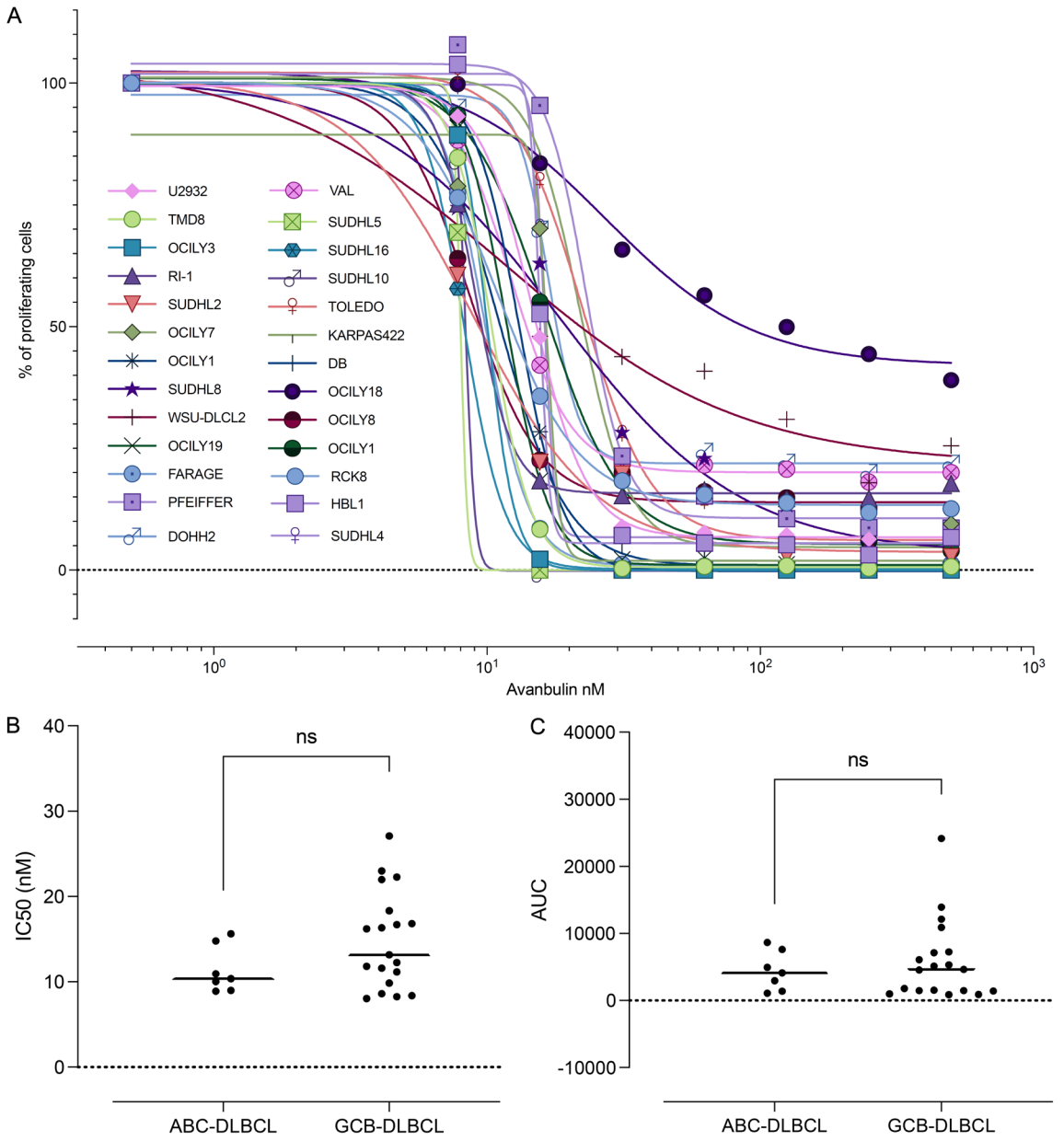

Figure 1. Anti-lymphoma activity of Avanbulin in diffuse large B cell lymphoma cell lines. (A) Dose response curve of avanbulin in 26 human diffuse large B-cell lymphoma cell lines after 72 hours of treatment. (B) IC50s and (C) area under the curve comparison between ABC and GCB-DLBCL cell lines. *P*-values obtained using the Mann-Whitney test.

(Supplementary Figure 6; Supplementary Table 4).

EB1 and MYC expression in DLBCL clinical specimens

We then assessed EB1 RNA expression in DLBCL clinical specimens. The transcript was highly expressed in most of the clinical specimens, with no difference based on the cell of origin (**Figure 3**). In agreement with what was seen in cell lines, we did not observe any correlation between EB1 RNA expression and MYC RNA expression and no association between EB1 expression and the presence of *MYC* translocation (**Figure 3**).

Finally, we looked at EB1 protein expression by immunohistochemistry (IHC) in DLBCL clinical specimens. On a total of 101 cases analyzed

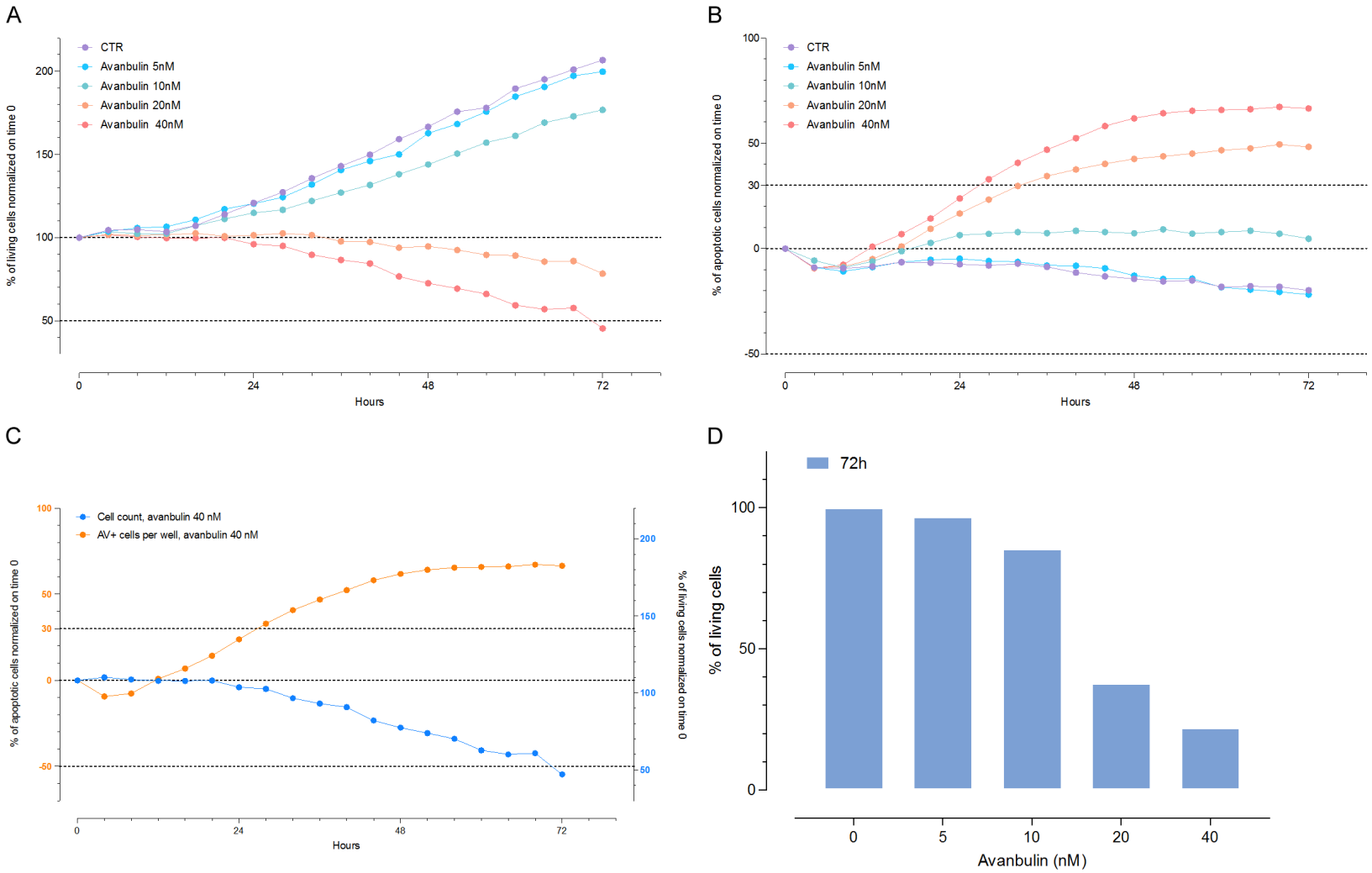

Figure 2. Antiproliferative activity and apoptosis induction of Avanbulin. Representative live cell imaging analysis performed in U2932 cell line. Cells under avanbulin treatment (5, 10, 20, 40 nM) compared to untreated cells. A. Cell growth at different time points under avanbulin treatment. B. Apoptosis induction during treatment measured as percentage of apoptotic cells normalized at the beginning of the treatment. C. Comparison of cell growth and apoptosis induction at 40 nM. D. Percentage of living cells at 72 hours normalized on untreated cells.

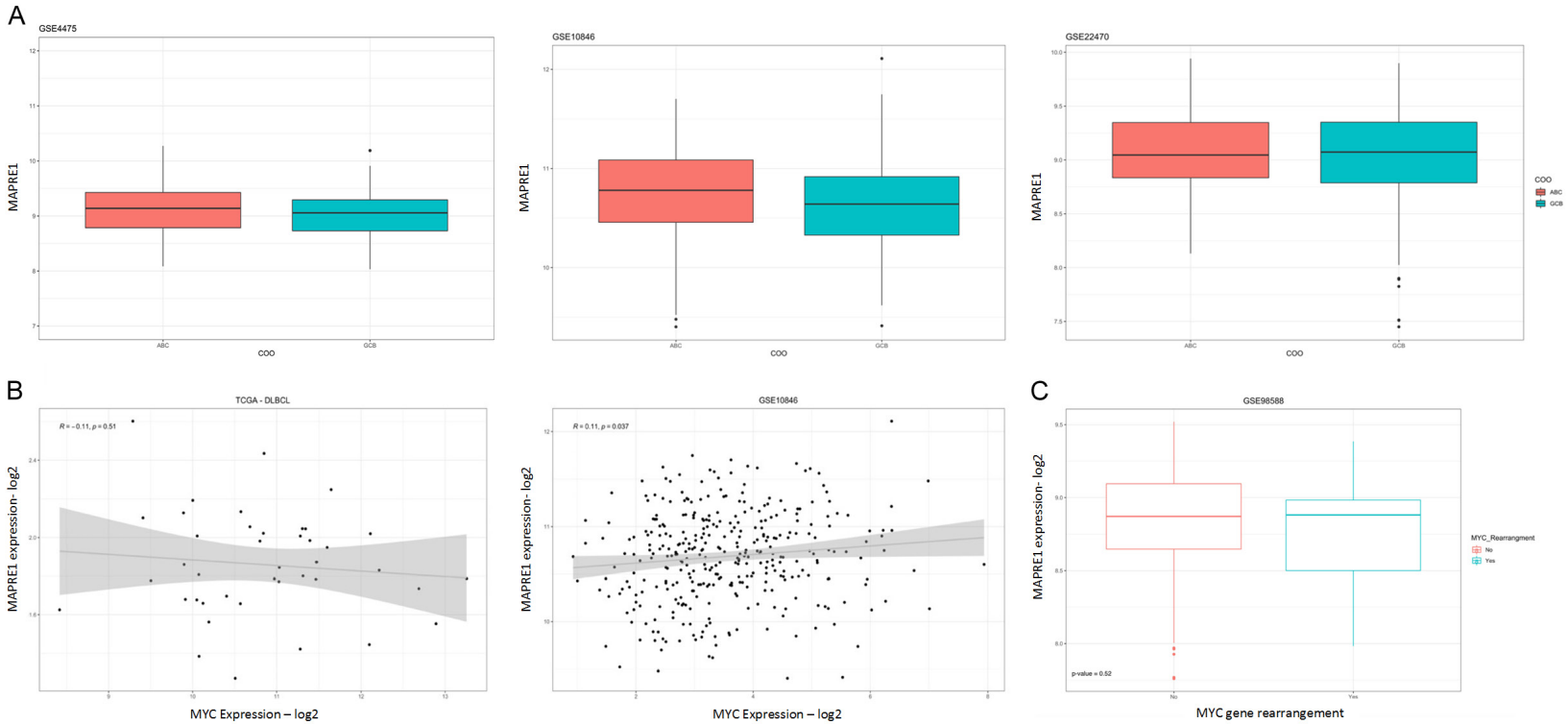

Figure 3. MAPRE-1 (EB1) RNA expression in DLBCL clinical specimens and correlation with MYC. A. MAPRE-1 (EB1) RNA expression in DLBCL clinical specimens divided by ABC (red) and GCB (blue) DLBCL. Three different datasets analyzed (GSE4475, GSE10846, GSE22470). B. Correlation between EB1 (MAPRE1 gene) expression and MYC expression in TCGA and GSE10846 datasets. C. MAPRE-1 expression levels in DLBCL clinical specimen divided between MYC without (red) or with (blue) rearrangements.

on TMAs, 51 were positive (50.5%) and 50 negative (49.5%) (Supplementary Table 5). Two percent of the tumor samples exhibited a moderate or strong EB1 staining in >50% of the tumor cells, 11% in 26-50% and 38% in 5-25%. In agreement with transcriptomes data, also by immunohistochemistry no difference between cell of origin was observed (Supplementary Figure 7).

Discussion

Here, we showed that the MTA avanbulin (BAL27862), the active moiety of lisavanbulin (BAL101553), showed a potent *in vitro* antitumor activity in DLBCL, and that the microtubule associated protein EB1, a potentially predictive biomarker of sensitivity to the compounds, was highly expressed in both DLBCL cell lines and clinical specimens.

Avanbulin showed a median IC50 of 11 nM across 26 DLBCL cell lines after 72 hours of drug exposure. The activity was mostly cytotoxic as confirmed by both cell cycle analysis and apoptosis assays. Real-time quantitative live-cell imaging allowed us to observe a fast decrease in cell proliferation and apoptosis induction. Around half of the cell lines tested had apoptosis induction in the first 24 hours of treatment; the remaining half after one additional day of drug exposure. Apoptosis was preceded by G2/M arrest. Out of 17 cell lines tested 15 presented apoptosis induction already at 20 nM. These data are in line with what is reported in solid tumor models [10-13], although our results were not further *in vivo* validated.

The microtubule-associated protein EB1 has been indicated as a potential biomarker of sensitivity to avanbulin and lisavanbulin, especially in the context of glioblastoma, in which a small number of cases express high protein levels, and these could be the cases that most benefit from treatment with the MTA [18, 20, 21]. In our DLBCL series, we did not see a clear correlation between EB1 expression and avanbulin anti-tumor activity, but only a trend for higher sensitivity in high EB1 expressor cell lines. Importantly, we detected high expression levels of EB1 at the RNA level in DLBCL cell lines and in DLBCL clinical specimens. Moreover, IHC indicated protein expression in 50% of DLBCL clinical specimens. Among the positive clinical specimens, 40% showed over 20% of the tumor cells highly positive with intensity of the staining between 2 and 3. Hence, based on this data, lisavanbulin is a promising agent to be tested in this population of patients. Moroever, we could not identify any relevant association between response to avanbulin and the presence of chromosomal translocations involving *BCL2* or *MYC* genes, or TP53 inactivation. With the limitations of the use of *in vitro* models, this observation suggests that also patients bearing these abnormalities might benefit from lisavanbulin.

Avanbulin binds to the colchicine site of tubulin and causes a destabilization of microtubules [9, 12]. Although the effect of avanbulin on microtubules phenotypically differs from that caused by vinblastine [9, 12], lymphoma cells are highly sensitive to microtubule destabilizers, including vinblastine itself, vincristine and MMAE. Our data suggest that DLBCL patients could potentially benefit from lisavanbulin treatment. Moreover, since the avanbulin tubulin binding site differs from both vinca alkaloids and MMAE and it does not appear to be a MDR1 substrate [5, 7, 9, 12, 14], lisavanbulin might be active also in patients that have developed resistance to these agents via tubulin mutations or MDR1 overexpression. A matter of concern for treating these patients is the potential overlapping toxicities, especially peripheral neuropathies, common to all MTAs [5, 8, 16-18], which might represent a limiting factor for using lisavanbulin in individuals already exposed to vincristine, vinblastine or antibody drug conjugates containing a MTA as payload. Keeping this possible toxicity in consideration, lisavanbulin might be first clinically explored in the context of patients with relapsed/refractory patients EB1 positive DLBCL after CAR T cells or that are unable to undergo the cellular therapies.

In conclusion, avanbulin showed strong antitumor activity in DLBCL cell lines and expression of its putative biomarker EB1 was observed in clinical specimens.

Acknowledgements

This project was partially supported by institutional research funds from Basilea Pharmaceutica International Ltd, Allschwil, Switzerland

and partially supported by the Swiss Cancer Research grant KFS-4713-02-2019. Thanks to Targos (Discovery Life Sciences Biomarker Services GmbH) for performing the EB1 IHC analysis.

Disclosure of conflict of interest

FB: institutional research funds from Acerta, ADC Therapeutics, Basilea Pharmaceutica, Bayer AG, Cellestia, CTI Life Sciences, Helsinn, ImmunoGen, Menarini Ricerche, NEOMED Therapeutics 1, Nordic Nanovector, Oncology Therapeutic Development, Oncternal Therapeutics, PIQUR Therapeutics; Spexis; consultancy fee from Helsinn, Menarini; expert statements provided to HTG; travel grants from Amgen, Astra Zeneca, Jazz Pharmaceuticals, PIQUR Therapeutics AG. NFG, FB, Marc Engelhardt, HL: employee of Basilea Pharmaceutica International Ltd, Basel, Switzerland.

Address correspondence to: Francesco Bertoni, Institute of Oncology Research, Faculty of Biomedical Sciences, USI, Via Francesco Chiesa 5, Bellinzona 6500, Switzerland. Tel: +41-58-666-7206; E-mail: francesco.bertoni@ior.usi.ch

References

[1] Alberts B, Bray D, Lewis J, Raff M, Roberts K and Watson J. Molecular Biology of the Cell. 3rd ed. New York: Garland Publishing, Inc.; 1994. pp. 1294.

[2] Nogales E, Whittaker M, Milligan RA and Downing KH. High-resolution model of the microtubule. Cell 1999; 96: 79-88.

[3] Nogales E, Wolf SG and Downing KH. Structure of the alpha beta tubulin dimer by electron crystallography. Nature 1998; 391: 199-203.

[4] Johnson KA and Borisy GG. Kinetic analysis of microtubule self-assembly in vitro. J Mol Biol 1977; 117: 1-31.

[5] Barreca M, Stathis A, Barraja P and Bertoni F. An overview on anti-tubulin agents for the treatment of lymphoma patients. Pharmacol Ther 2020; 211: 107552.

[6] Wordeman L and Vicente JJ. Microtubule targeting agents in disease: classic drugs, novel roles. Cancers (Basel) 2021; 13: 5650.

[7] McLoughlin EC and O'Boyle NM. Colchicine-binding site inhibitors from chemistry to clinic: a review. Pharmaceuticals (Basel) 2020; 13: 8.

[8] Barreca M, Lang N, Tarantelli C, Spriano F, Barraja P and Bertoni F. Antibody-drug conjugates for lymphoma patients: preclinical and clinical evidences. Explor Target Antitumor Ther 2022; 3: 763-795.

[9] Prota AE, Danel F, Bachmann F, Bargsten K, Buey RM, Pohlmann J, Reinelt S, Lane H and Steinmetz MO. The novel microtubule-destabilizing drug BAL27862 binds to the colchicine site of tubulin with distinct effects on microtubule organization. J Mol Biol 2014; 426: 1848-1860.

[10] Duran GE, Lane H, Bachmann F and Sikic BI. Abstract 4412: in vitro activity of the novel tubulin active agent BAL27862 in MDR1(+) and MDR1(-) human breast and ovarian cancer variants selected for resistance to taxanes. Cancer Res 2010; 70: 4412.

[11] Sharma A, Broggini-Tenzer A, Vuong V, Messikommer A, Nytko KJ, Guckenberger M, Bachmann F, Lane HA and Pruschy M. The novel microtubule targeting agent BAL101553 in combination with radiotherapy in treatment-refractory tumor models. Radiother Oncol 2017; 124: 433-438.

[12] Bachmann F, Burger K, Pohlmann J, Kellenberger L and Lane H. Abstract C229: BAL27862: a novel anticancer agent which dissociates microtubules and creates a distinct cellular phenotype. Mol Cancer Ther 2009; 8: C229.

[13] Esteve MA, Honore SP, Mckay N, Bachmann F, Lane H and Braguer D. Abstract 1977: BAL27862: a unique microtubule-targeted drug that suppresses microtubule dynamics, severs microtubules, and overcomes Bcl-2- and tubulin subtype-related drug resistance. Cancer Res 2010; 70: 1977.

[14] Pohlmann J, Bachmann F, Gertsch J, Altmann KH and Heim J. BAL27862: a novel oral tubulin interacting agent that overcomes the Pgp-related multidrug resistance phenotype in vitro and in vivo. Cancer Res 2007; 67: 1428.

[15] Pohlmann J, Bachmann F, Schmitt-Hoffmann A, Gebhardt K, Spickermann J, Nuoffer C, Biringer Gr, O'Reilly T, Pruschy M and Lane HA. Abstract 1347: BAL101553: an optimized prodrug of the microtubule destabilizer BAL27862 with superior antitumor activity. Cancer Res 2011; 71: 1347.

[16] Joerger M, Stathis A, Metaxas Y, Hess D, Mantiero M, Mark M, Volden M, Kaindl T, Engelhardt M, Larger P, Lane H, Hafner P, Levy N, Stuedeli S, Sessa C and von Moos R. A phase 1 study of BAL101553, a novel tumor checkpoint controller targeting microtubules, administered as 48-h infusion in adult patients with advanced solid tumors. Invest New Drugs 2020; 38: 1067-1076.

[17] Kristeleit R, Evans J, Molife LR, Tunariu N, Shaw H, Slater S, Haris NRM, Brown NF, Forster MD, Diamantis N, Rulach R, Greystoke A,

Asghar U, Rata M, Anderson S, Bachmann F, Hannah A, Kaindl T, Lane HA, Larger PJ, Schmitt-Hoffmann A, Engelhardt M, Tzankov A, Plummer R and Lopez J. Phase 1/2a trial of intravenous BAL101553, a novel controller of the spindle assembly checkpoint, in advanced solid tumours. Br J Cancer 2020; 123: 1360-1369.

[18] Tiu C, Tzankov A, Plummer R, Rulach R, Vivanco I, Mulholland PJ, Gurel B, Figueiredo I, Haris NM, Anderson S, Bachmann F, Engelhardt M, Kaindl T, Lane H, Litherland K, Pognan C, Berezowska S, Evans J, Kristeleit R and Lopez JS. 382P The potential utility of end-binding protein 1 (EB1) as response-predictive biomarker for lisavanbulin: final results from a phase I study of lisavanbulin (BAL101553) in adult patients with recurrent glioblastoma (GBM). Ann Oncol 2020; 31: S404.

[19] Joerger M, Hundsberger T, Haefliger S, von Moos R, Hottinger AF, Kaindl T, Engelhardt M, Marszewska M, Lane H, Roth P and Stathis A. Safety and anti-tumor activity of lisavanbulin administered as 48-hour infusion in patients with ovarian cancer or recurrent glioblastoma: a phase 2a study. Invest New Drugs 2023; 41: 267-275.

[20] Skowronska M, Tiu CD, Tzankov A, König F, Lewis J, Vivanco I, Kleinschmidt M, Beebe K, Anderson S, Bachmann F, Engelhardt M, Lane HA, Kaindl T, Stan AC, Plummer ER, Evans TRJ, Zlobec I and Lopez JS. Expression of end-binding protein 1 (EB1), a potential response-predictive biomarker for lisavanbulin, in glioblastoma and various other solid tumor types. J Clin Oncol 2021; 39: 3118-3118.

[21] Bergès R, Tchoghandjian A, Sergé A, Honoré S, Figarella-Branger D, Bachmann F, Lane HA and Braguer D. EB1-dependent long survival of glioblastoma-grafted mice with the oral tubulin-binder BAL101553 is associated with inhibition of tumor angiogenesis. Oncotarget 2020; 11: 759-774.

[22] Tirnauer JS and Bierer BE. EB1 proteins regulate microtubule dynamics, cell polarity, and chromosome stability. J Cell Biol 2000; 149: 761-766.

[23] Spriano F, Gaudio E, Cascione L, Tarantelli C, Melle F, Motta G, Priebe V, Rinaldi A, Golino G, Mensah AA, Aresu L, Zucca E, Pileri S, Witcher M, Brown B, Wahlestedt C, Giles F, Stathis A and Bertoni F. Antitumor activity of the dual BET and CBP/EP300 inhibitor NEO2734. Blood Adv 2020; 4: 4124-4135.

[24] Boi M, Gaudio E, Bonetti P, Kwee I, Bernasconi E, Tarantelli C, Rinaldi A, Testoni M, Cascione L, Ponzoni M, Mensah AA, Stathis A, Stussi G, Riveiro ME, Herait P, Inghirami G, Cvitkovic E, Zucca E and Bertoni F. The BET bromodomain inhibitor OTX015 affects pathogenetic pathways in preclinical B-cell tumor models and synergizes with targeted drugs. Clin Cancer Res 2015; 21: 1628-1638.

[25] Gaudio E, Tarantelli C, Spriano F, Guidetti F, Sartori G, Bordone R, Arribas AJ, Cascione L, Bigioni M, Merlino G, Fiascarelli A, Bressan A, Adjeiwaa Mensah A, Golino G, Lucchini R, Bernasconi E, Rossi D, Zucca E, Stussi G, Stathis A, Boyd RS, Dusek RL, Bisht A, Attanasio N, Rohlff C, Pellacani A, Binaschi M and Bertoni F. Targeting CD205 with the antibody drug conjugate MEN1309/OBT076 is an active new therapeutic strategy in lymphoma models. Haematologica 2020; 105: 2584-2591.

[26] Johnson Z, Tarantelli C, Civanelli E, Cascione L, Spriano F, Fraser A, Shah P, Nomanbhoy T, Napoli S, Rinaldi A, Niewola-Staszkowska K, Lahn M, Perrin D, Wenes M, Migliorini D, Bertoni F, van der Veen L and Di Conza G. IOA-244 is a non-ATP-competitive, highly selective, tolerable phosphoinositide 3-kinase delta inhibitor that targets solid tumors and breaks immune tolerance. Cancer Res Commun 2023; 3: 576-591.

[27] Huber W, Toedling J and Steinmetz LM. Transcript mapping with high-density oligonucleotide tiling arrays. Bioinformatics 2006; 22: 1963-1970.

[28] Irizarry RA, Bolstad BM, Collin F, Cope LM, Hobbs B and Speed TP. Summaries of affymetrix geneChip probe level data. Nucleic Acids Res 2003; 31: e15.

[29] Gentleman RC, Carey VJ, Bates DM, Bolstad B, Dettling M, Dudoit S, Ellis B, Gautier L, Ge Y, Gentry J, Hornik K, Hothorn T, Huber W, Iacus S, Irizarry R, Leisch F, Li C, Maechler M, Rossini AJ, Sawitzki G, Smith C, Smyth G, Tierney L, Yang JY and Zhang J. Bioconductor: open software development for computational biology and bioinformatics. Genome Biol 2004; 5: R80.

[30] Dobin A, Davis CA, Schlesinger F, Drenkow J, Zaleski C, Jha S, Batut P, Chaisson M and Gingeras TR. STAR: ultrafast universal RNA-seq aligner. Bioinformatics 2013; 29: 15-21.

[31] Anders S, Pyl PT and Huber W. HTSeq--a Python framework to work with high-throughput sequencing data. Bioinformatics 2015; 31: 166-169.

[32] Robinson MD, McCarthy DJ and Smyth GK. edgeR: a Bioconductor package for differential expression analysis of digital gene expression data. Bioinformatics 2010; 26: 139-140.

[33] Schmitz R, Wright GW, Huang DW, Johnson CA, Phelan JD, Wang JQ, Roulland S, Kasbekar M, Young RM, Shaffer AL, Hodson DJ, Xiao W, Yu X, Yang Y, Zhao H, Xu W, Liu X, Zhou B, Du W, Chan WC, Jaffe ES, Gascoyne RD, Connors JM,

Campo E, Lopez-Guillermo A, Rosenwald A, Ott G, Delabie J, Rimsza LM, Tay Kuang Wei K, Zelenetz AD, Leonard JP, Bartlett NL, Tran B, Shetty J, Zhao Y, Soppet DR, Pittaluga S, Wilson WH and Staudt LM. Genetics and pathogenesis of diffuse large B-cell lymphoma. N Engl J Med 2018; 378: 1396-1407.

[34] Whitaker RH and Placzek WJ. Regulating the BCL2 family to improve sensitivity to microtubule targeting agents. Cells 2019; 8: 346.

[35] Chang JT, Chang GC, Ko JL, Liao HY, Liu HJ, Chen CC, Su JM, Lee H and Sheu GT. Induction of tubulin by docetaxel is associated with p53 status in human non small cell lung cancer cell lines. Int J Cancer 2006; 118: 317-325.

[36] Giannakakou P, Sackett DL, Ward Y, Webster KR, Blagosklonny MV and Fojo T. p53 is associated with cellular microtubules and is transported to the nucleus by dynein. Nat Cell Biol 2000; 2: 709-717.

[37] Alexandrova N, Niklinski J, Bliskovsky V, Otterson GA, Blake M, Kaye FJ and Zajac-Kaye M. The N-terminal domain of c-Myc associates with alpha-tubulin and microtubules in vivo and in vitro. Mol Cell Biol 1995; 15: 5188-5195.

[38] Yang W, Soares J, Greninger P, Edelman EJ, Lightfoot H, Forbes S, Bindal N, Beare D, Smith JA, Thompson IR, Ramaswamy S, Futreal PA, Haber DA, Stratton MR, Benes C, McDermott U and Garnett MJ. Genomics of Drug Sensitivity in Cancer (GDSC): a resource for therapeutic biomarker discovery in cancer cells. Nucleic Acids Res 2013; 41: D955-961.

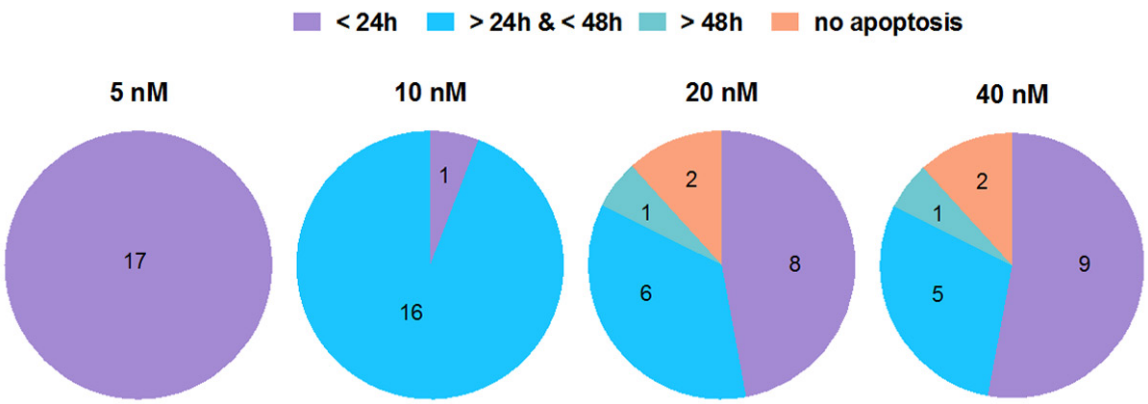

Supplementary Figure 1. Number of cell lines with Annexin V induction. Pie chart representing the number of cell lines undergoing apoptosis at different concentrations. Cells were divided based on the kinetics of apoptosis: no apoptosis, before 24, between 24 and 48 or later than 48 hours of treatment. Induction of apoptosis as >30% of apoptotic events compared to untreated cells by Incucyte.

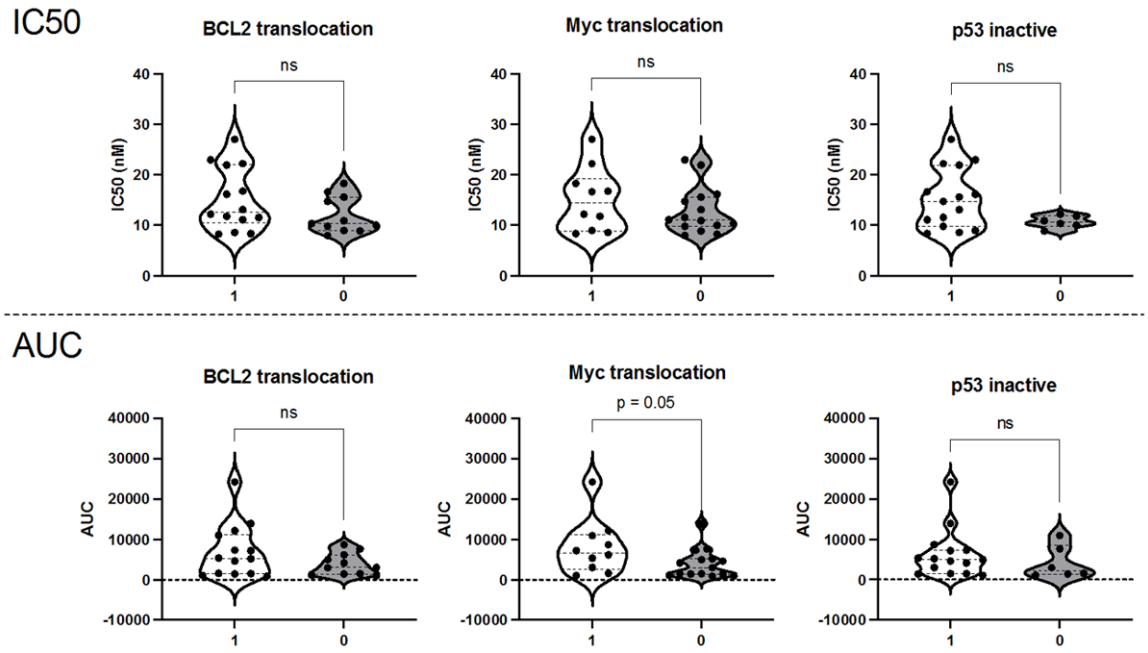

Supplementary Figure 2. Association between sensitivity and MYC or BCL2 or TP53 status. Association between IC50s or area under the curve (AUC) and MYC or BCL2 or TP53 status. 0 = wild type; 1 = altered status (translocation or inactivation). *P*-values obtained using the Mann-Whitney test.

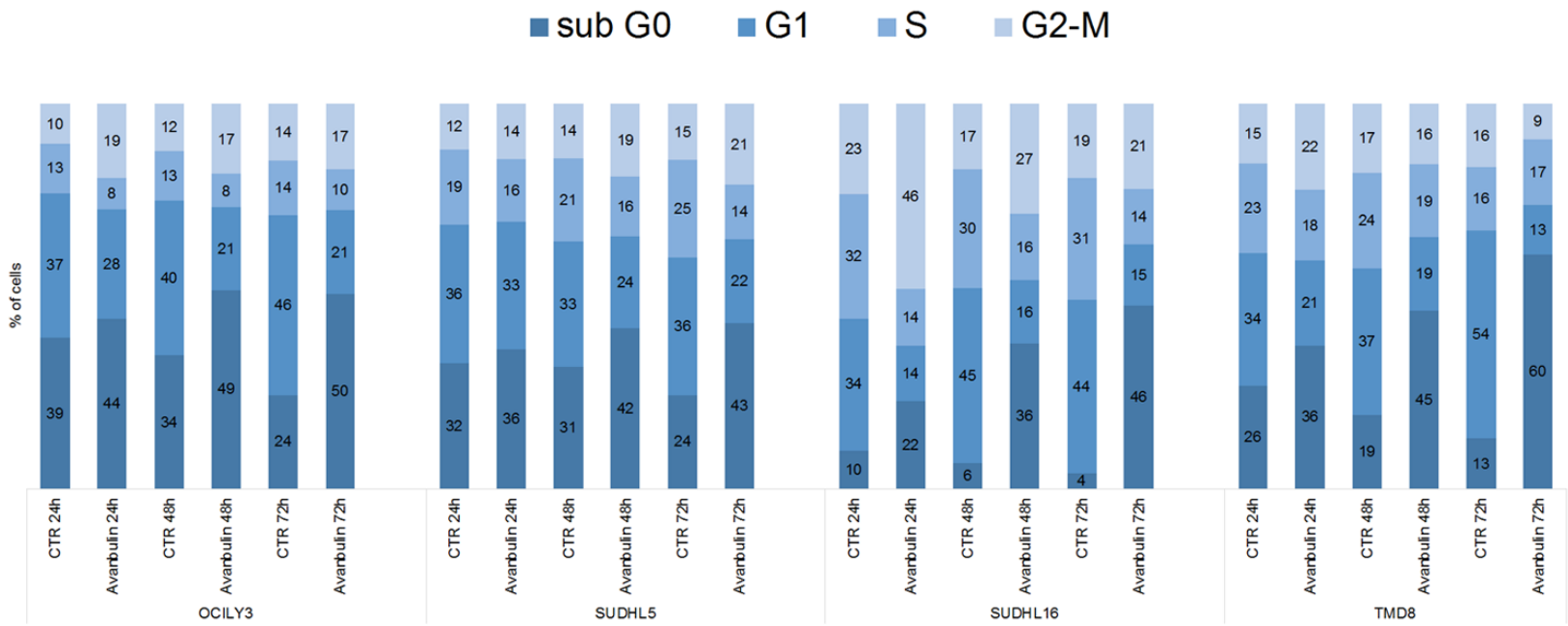

Supplementary Figure 3. Cell cycle analysis. Cell cycle analysis in four diffuse large B cell lymphoma cell lines after 24, 48 and 72 hours of treatment with 20 nM of avanbulin. Average of at least two independent experiments.

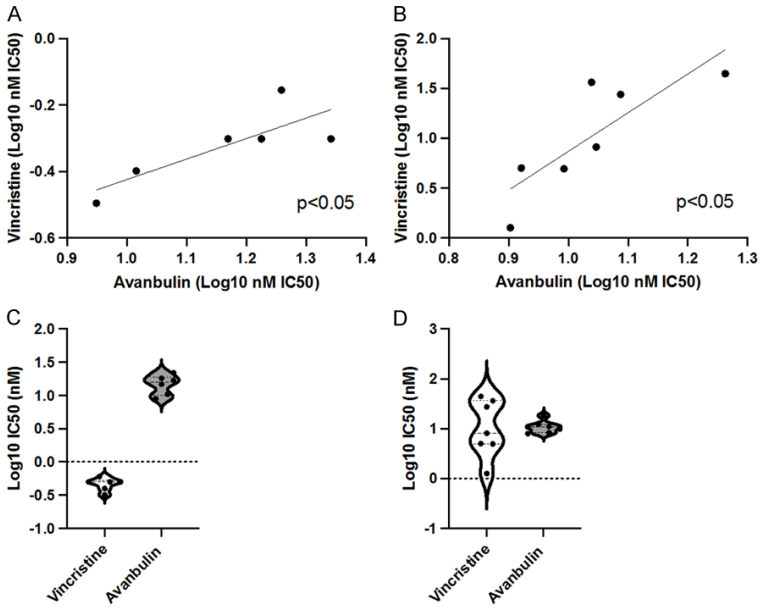

Supplementary Figure 4. Activity comparison between vincristine and avanbulin. Pearson correlation between avanbulin IC50 values and internal (A) or publicly available (B) vincristine IC50 values. Comparisons between avanbulin IC50 values and internal (C) or publicly available (D) vincristine IC50 values.

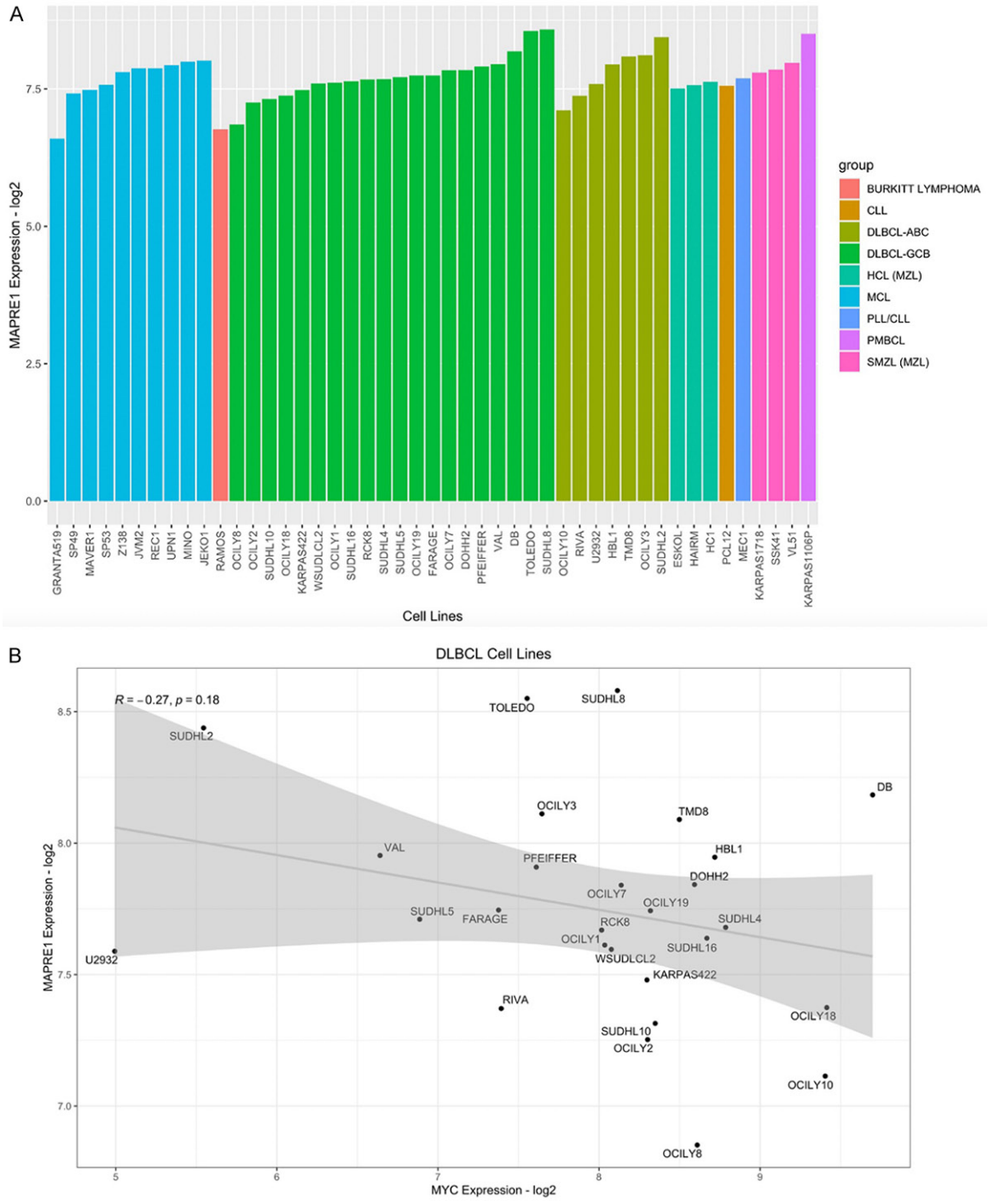

Supplementary Figure 5. EB1 expression in lymphoma cell lines. A. EB1 (MAPRE1 gene) expression level lymphoma cell lines divided by subtype. B. Correlation between EB1 and MYC expression in DLBCL cell lines.

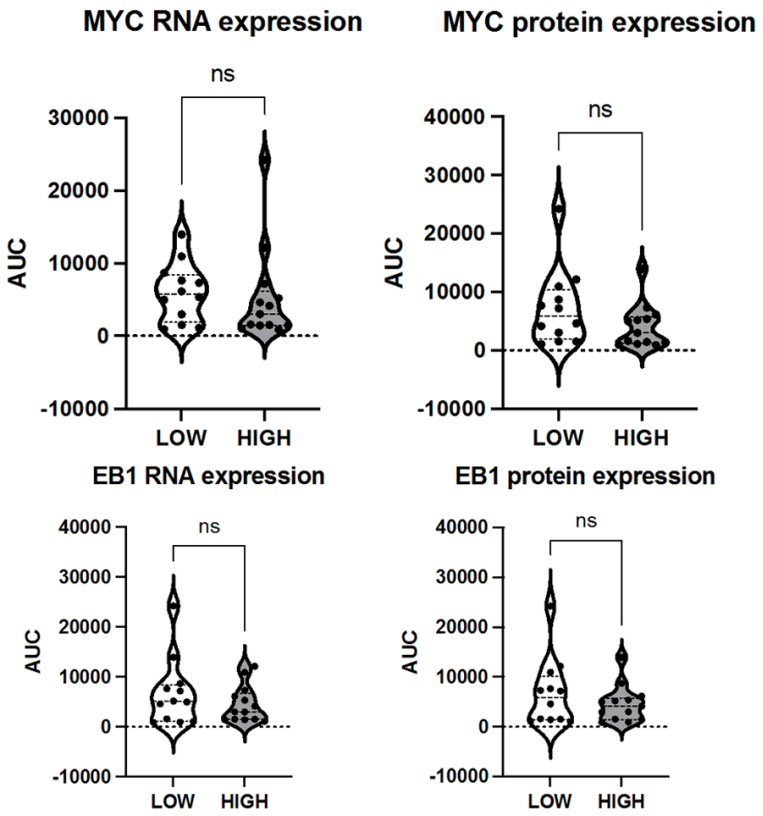

Supplementary Figure 6. EB1 and MYC expression in sensitive and resistant DLBCL cell lines. MYC and EB1 RNA or protein expression in cell lines with low (sensitive) or high (resistant) area under the curve (AUC). Cell lines were divided in low or high AUC if below or above the median AUC respectively. *P*-values obtained using the Mann-Whitney test.

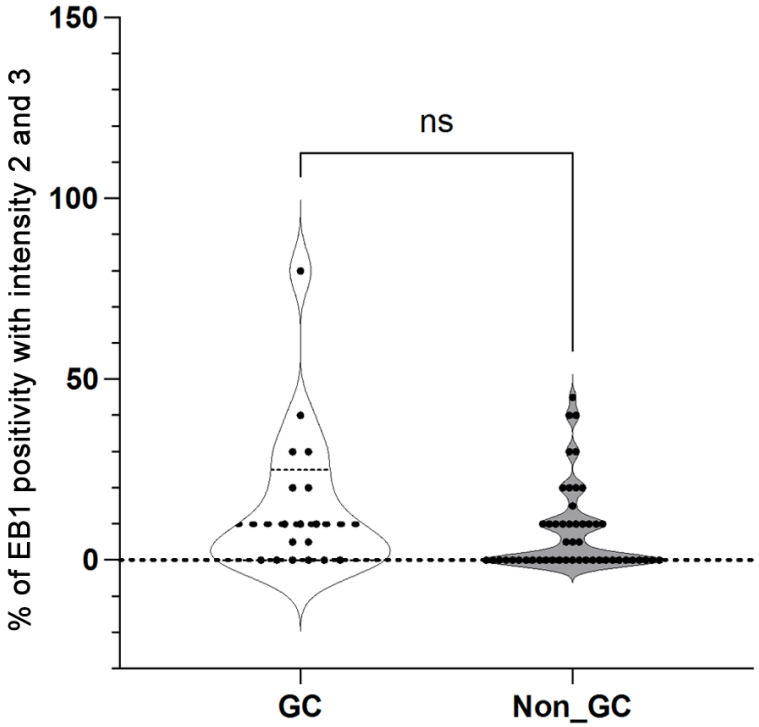

Supplementary Figure 7. Percentage of EB1 positivity by immunohistochemistry in germinal center (GC) versus non-germinal center DLBCLs patients. Y-axes shows the percentage of positivity with intensity 2 or 3 for each patient. Every dots represent one patient. *P*-values obtained using the Mann-Whitney test.